International Journal of Future Generation Communication and Networking
Vol. 9, No. 4 (2016), pp. 249-260
http://dx.doi.org/10.14257/ijfgcn.2016.9.4.22

# The Research of 3 D Point Cloud Registration Method Based On Regular Hexahedron Color Targets

Yu Guang, Shi Yunbo and Yu Boyang

*Measuring and Control Technology and Instrumentations*
*Harbin University of Science and Technology,*
*Harbin, China*
*E-mail: yuguang@hrbust.edu.cn, Shiyunbo@126.com*

***Abstract***

*Coded structured light measurement is the important method of modern non-contact optical measurement, restricted by the camera field of view, the surfaces to be measured can complete a single perspective measurement, this is the 3 d point cloud registration, point cloud registration can reflect three-dimensional topography on the surface of the object, and it has reached the requirement of comprehensiveness.This paper has built coded structured light 3 d measurement system, to explore 3 d point cloud registration method based on regular hexahedron color targets with high accuracy, fast registration, which can be applied to industrial components comprehensive measuring characteristics.*

***Keywords**: Coded Light, 3 D Measurement, Point Cloud Registration, Regular Hexahedron Color Target*

## 1. Introduction

Coded structured light measurement has been an important method in modern measurement technology. It is different with traditional contact measurement, which avoid the slight damage by measured object contact. However, for some large measured object, the single measurement range is small because of the limit about camera measuring field range. It can not do the omnibearing measurement in one time. Block measurement would be the only way. Unifying the several local measurement data into one coordinate system, which is 3 d point cloud registration. Therefore, 3 d point cloud registration is the key technology which can realize the large scale workpiece surface topography measurement.

Today, there are several high accuracy splicing method. They are precision mechanical splicing, electromagnetic tracker splicing, laser tracker splicing and marked point registration. These methods stitching accuracy are about $0.Xmm$. The accuracy is similar with shape measurement of encoding device. According to the characteristic of object reconstruction, this paper raises a kind of registration based on auxiliary stereo target. This method does not introduce other positioning devices. It can assure the surface information is complete. Besides, it is high efficiency and high accuracy. It can realize the registration of point clouds.

## 2. Key Technology of Image Processing in Registration

Each surface of color stereo target in this paper is color board. Using corner of the board to be the index point. These angular points need to be detected. Using Harris algorithm to do the corner detection and doing the experimental verification. When the camera shots picture, the color target would make the color deviation because of the peripheral environment some factors of camera. This paper designs the coupling

ISSN: 2233-7857 IJFGCN
Copyright ⓒ 2016 SERSC

correction based on hardware color and unbalance correction based on light intensity. The experiments verify its feasibility.

### 2.1 Index Point Location in Single Face

In the process of corner detection, what it's all about is to solve the change problems of longitudinal and transverse gray scale. Comparing white with black, bright color with dark color and color with white, which could be used in detection method.

The horizontal direction is X-axis and vertical direction is Y-axis. As is shown in figure 1. It defines the concept of frame, angular point and slip zone.

Frame (Gray circle): a little displace only in X-axis or Y-axis which makes gray level huge change.

Angular point (Black circle): a little displace both in X-axis and Y-axis which makes gray level huge change.

slip zone (White circle): a little displace both in X-axis and Y-axis which makes gray level little change.

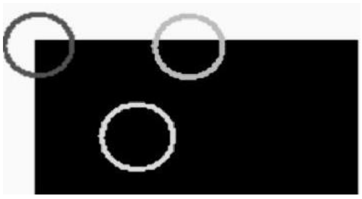

**Figure 1. Definition Chart of Angular Point**

Harris algorithm steps:

(1)Calculating matrix $M$ .

$$M = \begin{pmatrix} I_x^2 & I_x I_y \\ I_x I_y & I_y^2 \end{pmatrix} \quad (1)$$

$I_x$ is the gradient of pixel along the horizontal axis. $I_y$ is the gradient of pixel along the vertical axis.

(2)Doing Gauss smoothing.

$$w = \exp(-\frac{x^2 + y^2}{2\sigma^2}) \quad (2)$$

(3)Calculating corner response function value of pixel point in previous restore pictures. It is the value of $R(x, y)$ .

$$R = \left[I_x^2 \times I_y^2 - (I_x^2 I_y^2)\right] - k\left[I_x^2 + I_y^2\right]^2 \quad (3)$$

(4)Choosing the extreme point in the range of image and doing the range non maximum suppression.

(5)Setting a range $F$ . Detecting the angular point.

According to the principle of Harris algorithm, doing the program design. Making the simulation experiment in matlab, which is shown in figure 2. Extracting the angular point to the real image. The effect is shown in figure 3.

 Copyright ⓒ 2016 SERSC

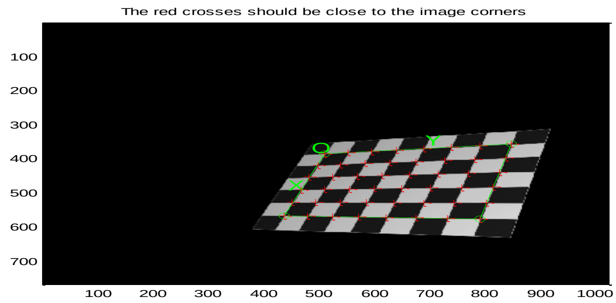


**Figure 2. Simulation Angular Point Detection**

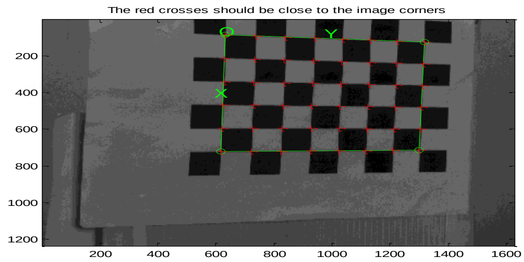


**Figure 3. Actual Angular Point Detection**

Choosing four angular point coordinates, which data is shown in table 1.

**Table 1. Angular Points Coordinate**

| | X | Y |
|---|---|---|
| 1 | 756.9279 | 103.9450 |
| 2 | 746.0027 | 277.9818 |
| 3 | 583.9277 | 140.8254 |
| 4 | 572.8869 | 264.3852 |

The experimental effect of angular points is good. It is accurate detection from visual perspective. Checking the accuracy according to gray fall method. The gray fall of V pixels around four angular points are greater than zero. It can prove the text is accuracy again.

### 2.2 Index Plane Distinguish

In this paper, the solid target is hexahedron. The color in six faces is different. Using standard color of palette in Windows XP system. The color is accuracy, which conveniences the identification behind.

The six faces color is: black, red, yellow, green, blue and violet. The bright lattice is white. It can distinguish six faces clearly in artificial vision. The RGB value in each color is different in computer vision. To identify each target surface, 2-3 target surfaces must do the color analysis from one point of view which camera shots.

The RGB value of six colors in color stereo target is: black(0,0,0), green(0,255,0), red(255,0,0), blue(0,0,255), yellow(255,255,0), violet(128,0,128), bright white(255,255,255). Doing the image processing from the difference of RGB. Measuring the RGB value of target image. It can fine out the accurate solid target surface.

Copyright ⓒ 2016 SERSC

When projecting full green encoding, a color component of horizontal pixel is shown in figure 4. From 4(a) and 4(b), images taken by camera would be mingled with red interference. It is color coupling in this paper. Red coupling would make huge effect to color reduction. therefore, color coupling correction need to be done before decoding.

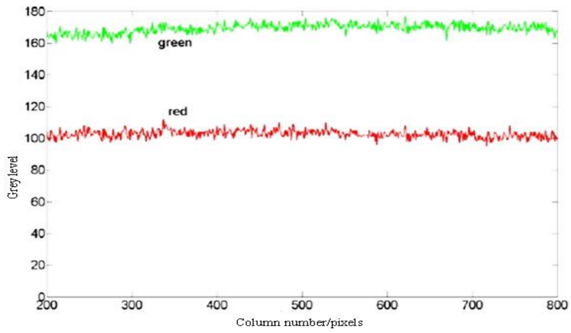


(a) Single green image

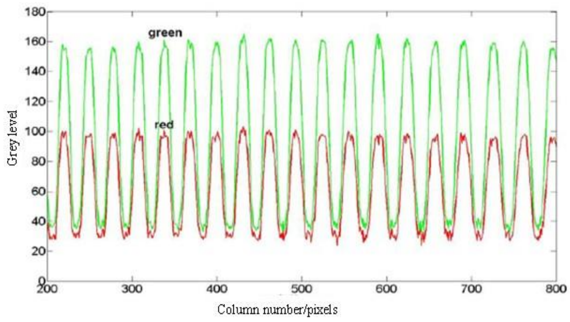


(B) Green-Red Stripe Image

**Figure 4. Color Coupling**

This paper designs the method of color reduction to solve that problem. Using color coupling images to do the calculates. Restoring non color coupling images before. This paper refer to the standard spectral plate in Windows XP and designs color reduction based on hardware. It is shown in formula 4. After correction, $W$ is image, $F$ is coupling coefficient, $Q$ is surface reflection parameters, $N$ is nonlinear transformation matrix, $W_1$ is projection pattern, $W_0$ is pending correction images.

$$\underbrace{\begin{bmatrix} R \\ G \\ B \end{bmatrix}}_{W} = \underbrace{\begin{bmatrix} f_{rr} & f_{rg} & f_{rb} \\ f_{gr} & f_{gg} & f_{gb} \\ f_{br} & f_{bg} & f_{bb} \end{bmatrix}}_{F} \underbrace{\begin{bmatrix} q_r & 0 & 0 \\ 0 & q_g & 0 \\ 0 & 0 & q_b \end{bmatrix}}_{Q} N \underbrace{\begin{bmatrix} r \\ g \\ b \end{bmatrix}}_{W_1} + \underbrace{\begin{bmatrix} R_0 \\ G_0 \\ B_0 \end{bmatrix}}_{W_0} \qquad (4)$$

Projecting five kinds of standard colors. The camera take pictures. Getting the parameters $W, F, Q, W_1, W_0$ from formula 4. Finally, using these parameters to structure correct color matrix.

Figure 5 is a heptachromic cylinder. It is distributed from the bottom up. Because of the physical form changing of object surface, light intensity of project encoding light and complicated peripheral environment, the reconstructed graph figure 5(b) is darker than figure 5(a) obviously. No matter how to translate and rotate this color cylinder, it can not change the color intensity error of figure 5(a) and figure 5(b) in restructure software. It causes the color imbalance.

 Copyright ⓒ 2016 SERSC

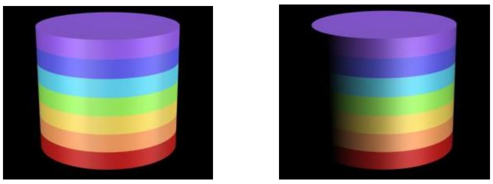

(a) Object Surface (b) Reconstructed Surface

**Figure 5. Color Unbalance**

Lots of reasons for affecting the light intensity deviation of object surface reflection and incidence. They are angle of arrival, angle of reflection and incident distance.

The project angle of reflection can be confirmed first. The incident light intensity ratio can be shown as formula 5.

$$Z = \frac{I_{i1}}{I_{i2}} = \frac{I_{iL1} \times I_{i\theta 1}}{I_{iL2} \times I_{i\theta 2}} = \frac{L_2^{\ 2} \times \sin^2 \theta_1}{L_1^{\ 2} \times \sin^2 \theta_2} \qquad (5)$$

Comparing the incident light intensity with the reflected light intensity, the color correction coefficient $C$ could be calculated. It is shown in formula 6.

$$C = \frac{L_2^{\ 2} \times \sin^2 \theta_1 \times \sin \gamma_1}{L_1^{\ 2} \times \sin^2 \theta_2 \times \sin \gamma_2} \qquad (6)$$

$\gamma_1, \gamma_2$ are reflection angle of two section. The color correction coefficient $C$ is the coefficient product of incident light intensity and reflected light intensity.

Using color coupling correction and color imbalance correction to do the color correction experiment respectively. The color information of sampling image is shown in figure 6. The sample color image is shown in figure 6(a). Doing the color correction experiment to a part. The color coupling correction based on hardware are shown in figure 6(b) and figure 6(c). The experimental data is root in figure 4.

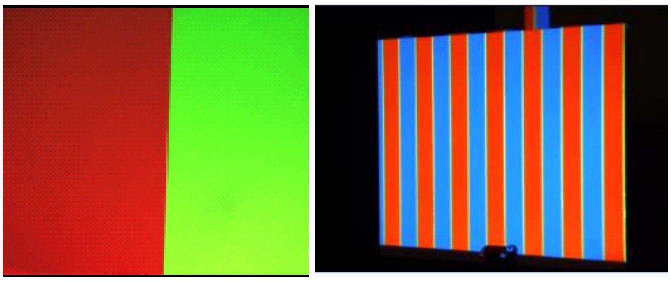

(a) Color Images

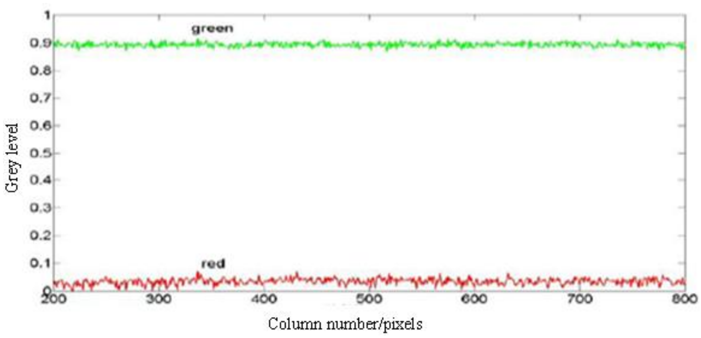


Copyright ⓒ 2016 SERSC

(b) Single green image

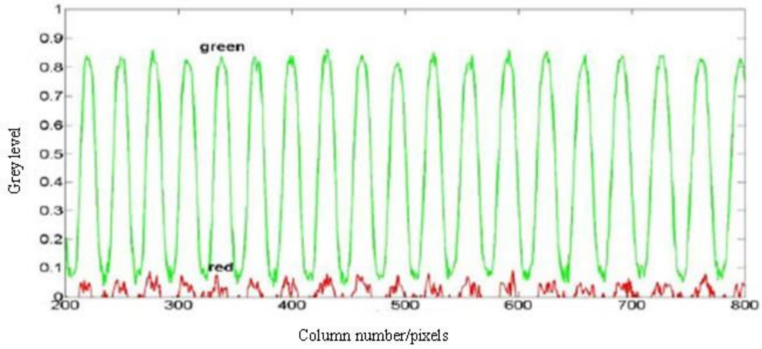


(c) Green-red stripe image

**Figure 6. Color Coupling Calibration**

From the experimental data, after correction, the color coupling error is 1/10 which before correction. Restore the color information of object itself basically. It proves the color coupling correction based on hardware in this paper is reasonable.

Being directed against the color imbalance, this paper designs intensity correction method. Making calibration experiment to a red surface. The experimental result is shown in table 2. $A_1$ is the value $R$ of this pixel before correction. $A_2$ is the value $R$ of this pixel after correction.

**Table 2. Samples Color Before and After Correction**

| Line number | Column number | Color | |
|---|---|---|---|
| | | $A_1$ | $A_2$ |
| 170 | 90 | 0.749 | 0.771 |
| 170 | 190 | 0.528 | 0.782 |
| 210 | 90 | 0.703 | 0.713 |
| 210 | 190 | 0.502 | 0.765 |
| 250 | 170 | 0.716 | 0.769 |
| 250 | 270 | 0.601 | 0.762 |
| 270 | 170 | 0.593 | 0.761 |
| 270 | 270 | 0.528 | 0.772 |
| 290 | 170 | 0.699 | 0.771 |
| 290 | 270 | 0.624 | 0.768 |

Before correcting, the difference between maximal value with minimum value of $R$ is bigger than 0.3. Artificial vision could distinguish this color imbalance deviation. After correcting, the difference between maximal value with minimum value of $R$ is smaller than 0.1. Artificial vision could not distinguish this color imbalance deviation. It level off to the resolution ratio of human eyes to the color component $R, G, B$.

## 3. Encoding the Light D Measurement and Splicing Appararatus Construction

The measurement system and splicing system is constituted by CCD camera, projector, computer and calculation software in this paper. Encoding light measurement system sketch map is shown in figure 7.

 Copyright ⓒ 2016 SERSC

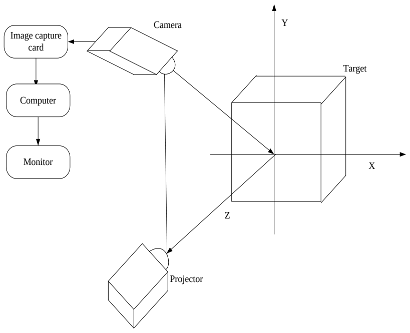


**Figure 7. The Measurement System Model Chart**

In the process of establishing measurement system and splicing system, there are two points need to be considered.

(1) The measurement space of measurement system is as bigger as possible, which is convenient to measure large volume object.

(2) Adjusting the camera and projector to an appropriate distance, which makes the images more clearer. It makes the post process convenient.

The actual encoding light measurement system device in condition of laboratory is shown in figure 8.

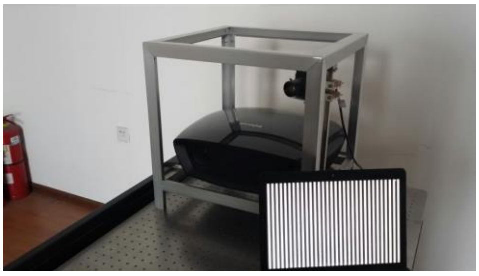

**Figure 8. Encoding Light Measurement System**

According to the actual camera coverage, this paper designs a normal cube as solid target of which the length is 80mm. It is shown in figure 9.

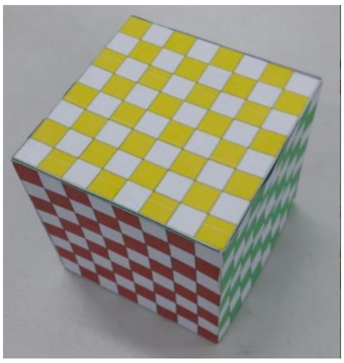

**Figure 9. Color Experimental Target**

In experiment, the flow chart of encoding light system detection is shown in figure 10.

Copyright ⓒ 2016 SERSC 


**Figure 10. Flow Chart of Encoding Light Detection**

# 4. Splicing Experiments

# 5.

## 4.1Qualitative Analysis of Splicing Experiments

In actual splicing experiment, the ceramic carving is selected to be detection target. Owing to the measuring range of encoding optical system and much too long target, It need to areal survey. As is shown in figure 11.

**Figure 11. The Detection Target**

Doing the encoding light measurement to the ceramic carving. The measurement is divided in to two parts: visual angle 1 and visual angle 2. As is shown in figure 12, figure 12(a) and figure 12(b) are the encoded image of visual angle 1 and visual angle 2. It can reflect each part of the measurement in two visual angle.

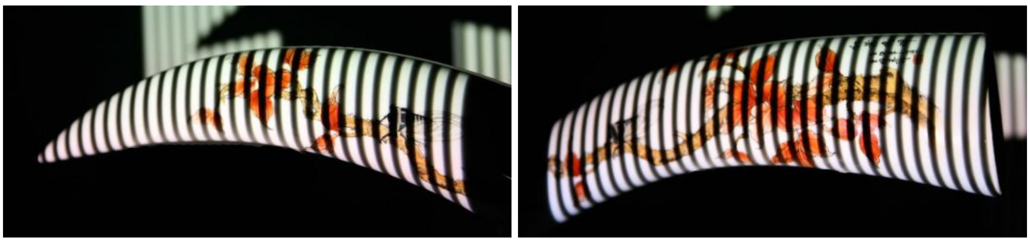

(a) Visual Angle 1 (b) Visual Angle 2

**Figure 12. Coding in Two Visual Angles**

Restructuring the measured ivory in two visual angle and getting the reconstructed images. It is shown in figure 13. Figure 13(a) is the reconfiguration of visual angle 1 and Figure 13(b) is the reconfiguration of visual angle 2.

 Copyright ⓒ 2016 SERSC

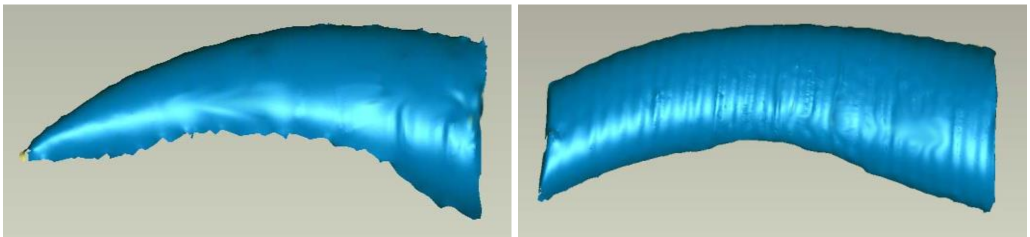

(a) Reconfiguration of Visual Angle 1 (B) Reconfiguration of Visual Angle 2

**Figure 13. Reconfiguration in Two Visual Angles**

According to 3 d point cloud registration, the image after split joint can be get. It is shown in figure 14.

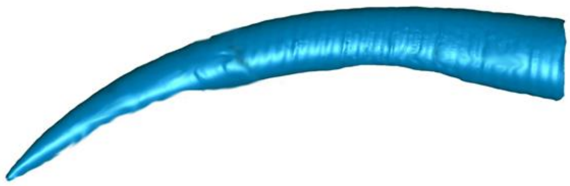

**Figure 14. The Image of Reconfiguration**

From figure 14, the stitching effect is good. It expresses the 3 d point cloud information ivory carving surface commendably, which reach the requirements of this paper.

### 4.2 Quantitative Analysis of Splicing Experiments

In actual experiment, it extracts the angular points of auxiliary stereo target face 2. There are 49 angular points in the surface of auxiliary stereo target. Selecting 5 angular points number 10, number 16, number 21, number 29, number 33 to be characteristic points. The index points order is named 1, 2, 3, 4, 5. Detecting the two-dimensional coordinates, which is shown in table 3.

**Table 3. Two Dimensional Image Coordinates**

| Index points | Visual angle 1 | | Visual angle 2 | |
|---|---|---|---|---|
| | X | Y | X | Y |
| 1 | 748.2561 | 108.2694 | 417.2548 | 130.2641 |
| 2 | 731.6947 | 269.4582 | 417.6649 | 279.4562 |
| 3 | 576.3561 | 139.6895 | 253.9421 | 158.1286 |
| 4 | 751.3845 | 281.5520 | 431.2045 | 290.0021 |
| 5 | 572.3664 | 138.6630 | 259.3662 | 154.2445 |

Converting the index point two dimensional coordinates to three dimensional coordinates. It is shown in table 4.

**Table 4. Three Dimensional Space Coordinates**

| Index points | Visual angle 1 | | | Visual angle 2 | | |
|---|---|---|---|---|---|---|
| | X | Y | Z | X | Y | Z |
| 1 | 107.2569 | 106.3215 | 35.2847 | -19.2556 | 99.0887 | 38.2214 |
| 2 | 101.2653 | 42.3659 | 30.0021 | -30.8417 | 42.5582 | 29.5541 |
| 3 | 61.2354 | 74.2159 | 59.6685 | -79.8542 | 90.3369 | 61.5564 |
| 4 | 98.2365 | 42.6812 | 31.5874 | -30.2669 | 40.1128 | 28.4421 |
| 5 | 47.8826 | 79.3220 | 70.2996 | -79.8441 | 90.4471 | 64.1101 |

Using the three-dimensional data of index points to do the coordinate transformation. Calculating the rotation matrix $R$ and translation matrix $T$, which are shown below:

$$R = \begin{bmatrix} 49.834 & 50.238 & 49.688 \\ 80.258 & 77.220 & 70.284 \\ 9.273 & 90.253 & 40.258 \end{bmatrix}$$

$$T = \begin{bmatrix} -80.280 \\ 70.399 \\ 39.258 \end{bmatrix}$$

After the experiment, Doing the arithmetic to the coincidence degree of five evaluation points. The results are shown in table 5.

**Table 5. Experimental Errors**

| | 1 | 2 | 3 | 4 | 5 |
|---|---|---|---|---|---|
| Labeling points method | 0.58 | 0.54 | 0.56 | 0.53 | 0.54 |
| Planar target method | 0.60 | 0.57 | 0.53 | 0.52 | 0.56 |
| Auxiliary stereo target method | 0.52 | 0.50 | 0.49 | 0.51 | 0.54 |

The stitching errors of three splicing methods are close to the error of encoding light measurement. The errors come from hardware and measurement environment.

From table 5, the auxiliary stereo target method is better than the other two traditional stitching methods. It proves the method raised in this paper is accurate and credible.

## 5. Conclusion

This paper raises the splicing method based on auxiliary stereo target. Designing a hexahedron color target. In the process of target surface distinguish, It utilizes Harris corner detection. The accuracy is validated by experiment. Besides, This paper designs coupled color correction based on hardware unbalanced color correction based on light intensity method, which accuracy is validated by experiment. Finally, using a ceramic carving to be a detection target. From experiment, The result of auxiliary stereo target method is better than which of two traditional method.

## References

[1] G. Chazan and N. Kiryati, "Pyramidal intensity-ratio depth sensor[R]", Technical Report, Center for Communication and Information Technologies, Department of Electrical Engineering, Technique, **(1995)**, Haifa, Israel.

[2] R. Yong, "3D Measurement Method by Combining RGB Gray Code with Trapezoidal Phase-shifting [D]", Journal of Harbin University of Science and Technology, **(2011)**.

 Copyright ⓒ 2016 SERSC

[3] C. Schmalz, F. Forster and A. Schick, “An endoscopic 3D scanner based on structured light[J]”, Medical image analysis, vol. 16, no. 5, **(2012)**, pp. 1063-1072.
[4] P. Mountney, D. Stoyanov and G. Z. Yang, “Three-dimensional tissue deformation recovery and tracking[J]”, Signal Processing Magazine, IEEE, vol. 27, no. 4, **(2010)**, pp. 14-24.
[5] H. Masuda and K. Fukuda, “Ordered metal nanohole arrays made by a two-step replication of honeycomb structures of anodic alumina [J]”, Science, vol. 268, no. 5216, **(1995)**, pp. 1466-1468.
[6] Y. Fang, K. Yamada and Y. Ninomiya, “A Shape-independent Method for Pedestrian Detection with Far-infrared Images [J]”, IEEE Transactions on Vehicular Technology, vol. 53, no. 6, **(2004)**, pp. 1679-1697.
[7] F. Bruno, G. Bianco and M. Muzzupappa, “Experimentation of structured light and stereo vision for underwater 3D reconstruction [J]”, ISPRS Journal of Photogrammetry and Remote Sensing, vol. 66, no. 4, **(2011)**, pp. 508-518.
[8] Z. Lin and L.S. Davis, “A Pose-invariant Descriptor for Human Detection and Segmentation [C]”, European Conference on Computer Vision, **(2008)**, pp. 423-436.
[9] T. Pribanić, S. Mrvoš and J. Salvi, “Efficient multiple phase shift patterns for dense 3D acquisition in structured light scanning [J]”, Image and Vision Computing, vol. 28, no. 8, **(2010)**, pp. 1255-1266.
[10] J.A.C. Yule, “Principles of color reproduction, applied to photomechanical reproduction, color photography, and the ink, paper, and other related Industries [M]”, **(1967)**, New York, Wiley.

 Copyright ⓒ 2016 SERSC